Electronic Supplementary Information

A 3D [WS$_4$Cu$_4$]$^{2+}$ cluster-based material with high iodine uptake capability

Meng-Di Liu,[ab] Brendan F. Abrahams,[c] Zhi-Gang Ren*[a] and Jian-Ping Lang*[ab]

[a] College of Chemistry, Chemical Engineering and Materials Science, Soochow University, Suzhou 215123, P. R. China

[b] State Key Laboratory of Organometallic Chemistry, Shanghai Institute of Organic Chemistry, Chinese Academy of Sciences, Shanghai 200032, P. R. China

[c] School of Chemistry, University of Melbourne, Victoria 3010, Australia

Table of Contents

Experimental

Materials and measurements. All chemicals and solvents used in the synthesis were of reagent grade from commercial source and employed without further purification. Elemental analyses (EA) for C, H, and N were determined on a Carlo-Erba CHON-S microanalyzer. Infrared (IR) spectra were recorded on a Thermo Electron Thermo Electron NEXUS 670 FT-IR spectrometer as KBr pellets (4000-400 cm^{-1}). UV-vis spectra were measured on a Shrmadzu UV-2600 UV-vis spectrophotometer. Thermogravimetric analyses (TGA) were performed under nitrogen atmosphere on a Mettler Toledo Star System. Powder X-ray diffraction (PXRD) patterns were collected on an X'Pert-Pro MPD diffractometer (Netherlands PANalytical) (Cu-Kα). The BET adsorption tests were implemented on the BELSORP-max (BEL, Japan) surface section and pore size analyzer. Scanning electron microscopy (SEM) images were carried on a HITACHI S-4700 cold field-emission scanning electron microscope.

Preparation of [WS$_4$Cu$_4$(μ-CN)$_2$(bpea)$_2$]·1.5DMF (1·1.5DMF). A 10 mL vial was added (NH$_4$)$_2$WS$_4$ (3.48 mg, 0.01 mmol), CuCN (3.58 mg, 0.04 mmol) and 2 mL DMF and then sealed. The mixture was thoroughly stirred for 2 h at room temperature. After a little orange precipitate was filtered off, the orange-yellow supernatant liquor was placed in a glass tube (30 cm in length, 6 mm in inner diameter). An additional 2 mL of DMF was carefully layered on the surface as a "buffer band". This was followed by the slow addition of bpea (3.68 mg, 0.02 mmol) in 2 mL DMF onto the buffer band. The glass tube was then sealed and allowed to stand at room temperature. Orange-red, prismatic crystals of **1**·1.5DMF were collected after several days, which were collected by filtration, washed with Et$_2$O and dried in air. Yield: 4.93 mg (45% based on W). Anal. Calcd (%) for C$_{61}$H$_{69}$Cu$_8$N$_{15}$O$_3$S$_8$W$_2$: C, 33.41; H, 3.17; N, 9.58. Found: C, 33.03; H, 3.465; N, 9.789. IR (KBr pellet, cm^{-1}): 3439.09 (s), 2919.76 (w), 2850.04 (w), 2135.89 (m), 1666.79 (m), 1607.76 (s), 1556.09 (w), 1499.04 (w), 1422.77 (m), 1384.27 (m), 1261.06 (w), 1067.57 (w), 1013.60 (w), 822.45 (m), 545.45 (w), 470.47 (w), 414.86 (w), 404.32 (w).

Preparation of [WS$_4$Cu$_4$(μ-CN)$_2$(bpea)$_2$]·3CH$_3$OH (1·3CH$_3$OH). As-synthesized crystals of **1**·1.5DMF were immersed in CH$_3$OH for 3 days. During this period, the solvent was renewed by fresh methanol every six hours. Thereafter, the methanol-exchanged crystals of **1**·3CH$_3$OH were collected by centrifugation, slightly washed with Et$_2$O and dried in air. Anal. Calcd (%) for

$C_{29}H_{36}Cu_4N_6O_3S_4W$: C, 32.17; H, 3.35; N, 7.76. Found: C, 33.21; H, 3.973; N, 7.621. IR (KBr pellet, cm^{-1}): 3418.39 (m), 2919.32 (w), 2850.71 (w), 2128.36 (s), 1608.52 (s), 1557.49 (w), 1498.02 (w), 1423.81 (s), 1384.57 (w), 1223.20 (w), 1118.44 (m), 1068.20 (w), 1013.78 (w), 822.88 (m), 619.48 (s), 544.41 (m), 438.99 (m), 411.89 (w), 406.01 (w), 400.22 (w).

Preparation of [WS$_4$Cu$_4$(μ-CN)$_2$(bpea)$_2$] (1·*des*). As-prepared crystals **1**·3CH$_3$OH were placed under vacuum at 60 °C for 12 h to obtain the desolvated crystalline solid **1**·*des*. Anal. Calcd (%) for $C_{26}H_{24}Cu_4N_6S_4W$: C, 31.65; H, 2.45; N, 8.52. Found: C, 31.32; H, 2.617; N, 8.629. IR (KBr pellet, cm^{-1}): 3450.26 (m), 2921.72 (w), 2851.55 (w), 2127.00 (m), 1608.64 (s), 155.65 (w), 1499.79 (w), 1423.86 (m), 1384.16 (m), 1223.40 (w), 1068.04 (w), 1014.10 (w), 819.13 (w), 544.45 (w), 438.90 (m), 419.64 (w), 403.81 (w), 400.19 (w).

Preparation of I$_2$@1 sample. The finely-ground crystals **1**·*des* (100 mg) were soaked in a 100 mL of cyclohexane solution containing 254 mg of iodine. After a week, the resulting black crystals were separated from the excess iodine solution and then dried in air. The final mass of crystals were weighted 210.56 mg, namely increased by 110.6 wt%. The adsorbed amount of iodine into the crystals was further estimated by thermogravimetric analysis (TGA).

Single-crystal X-ray crystallography. An X-ray quality orange-red prismatic single crystal was selected and coated with silicon grease. Single crystal measurements were undertaken on a Bruker D8-Quest CCD X-ray diffractometer equipped with graphite monochromated Mo Kα radiation (λ = 0.71073 Å) at 210 K. The Bruker APEX2 program was utilized to integrate all reflection datum and refine cell parameters. The adsorption was corrected using the SADABS routine.[S1-S3] The crystal structure was solved by direct methods and refined by the full-matrix least-squares method on F^2 utilizing the SHELXTL-2016 software programs.[S4] All non-hydrogen atoms were refined with anisotropic displacement parameters. The remaining organic hydrogen atoms were refined in geometrically calculated locations. Guest molecules were severely disordered, and could not be modelled. Diffuse electron density associated with the disordered solvent was eliminated using the SQUEEZE subprogram in PLATON package. The eventual formula was ascertained by the further elemental analysis and thermogravimetric analysis data. The atoms C1 and N1 from the cyanide anion, were refined with equal site occupancies of 50%, using EXYZ and EADP

commands in SHELXTL. Disorder in the phenyl groups was treated by applying site occupancies of 0.6 and 0.4 to identify the locations of C2, C3, C5 and C6. A summary containing the pertinent crystal data and structure refinement paprameters for **1**·1.5DMF is presented in Table S1 while its selected bond lengths (Å) and angles (°) are listed in Table S2.

Table S1 Crystal data and structure refinement parameters for **1**·1.5DMF.

Compound	**1**·1.5DMF
empirical formula	$C_{30.50}H_{34.50}Cu_4N_{7.50}O_{1.50}S_4W$
formula weight	1096.4
crystal system	Cubic
space group	*Ia-3d*
a/Å	30.6564(16)
b/Å	30.6564(16)
c/Å	30.6564(16)
V/Å^3	28811.34(500)
ρ_{calc}/g cm^{-3}	1.365
Z	24
μ/mm^{-1}	4.322
$F(000)$	11424
$R_1{}^a$	0.0753
$wR_2{}^b$	0.2442
GOF^c	1.116

$^aR_1 = \Sigma||F_o|-|F_c||/\Sigma|F_o|$. $^bwR_2 = \{\Sigma w(F_o{}^2-F_c{}^2)^2/\Sigma w(F_o{}^2)^2\}^{1/2}$. $^cGOF = \{\Sigma w((F_o{}^2-F_c{}^2)^2)/(n-p)\}^{1/2}$, where n = number of reflections and p = total number of parameters refined.

Table S2 Selected bond lengths (Å) and angles (º) for **1**·1.5DMF.

W(1)-S(1)	2.231(3)	W(1)-Cu(1)	2.6921(12)
Cu(1)-N(1)	1.933(10)	Cu(1)-C(1)	1.933(10)
Cu(1)-N(2)	2.126(10)	Cu(1)-S(1)	2.291(3)
Cu(1)-S(1)#1	2.295(3)		
S(1)-W(1)-S(1)#1	109.02(7)	S(1)-W(1)-S(1)#2	110.36(15)
S(1)#1-W(1)-S(1)#2	109.03(7)	S(1)-W(1)-S(1)#3	109.03(7)
S(1)#1-W(1)-S(1)#3	110.36(14)	S(1)#2-W(1)-S(1)#3	109.03(7)
N(1)-Cu(1)-N(2)	99.8(4)	C(1)-Cu(1)-N(2)	99.8(4)
N(1)-Cu(1)-S(1)	116.0(4)	C(1)-Cu(1)-S(1)	116.0(4)
N(2)-Cu(1)-S(1)	112.5(3)	C(1)-Cu(1)-S(1)#1	116.0(4)
N(2)-Cu(1)-S(1)#1	107.8(3)	S(1)-Cu(1)-S(1)#1	104.77(13)
Cu(1)-S(1)-Cu(1)#3	112.30(12)		

Symmetry transformations used to generate equivalent atoms: #1: $-z + 3/4$, $-y + 1/4$, $x - 3/4$; #2: $-x + 3/2$, y, $-z$; #3: $z + 3/4$, $-y + 1/4$, $-x + 3/4$.
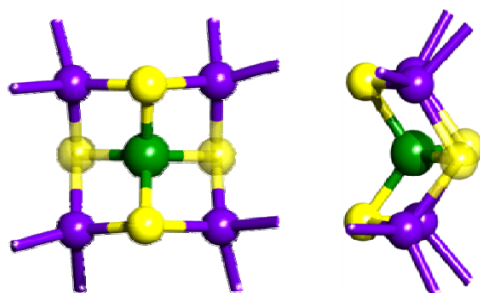
Fig. S1 View of the saddle-shaped $[WS_4Cu_4]^{2+}$ core from the *a* axis (left) and the *b* axis (right).

(a)	(b)

(c)	(d)
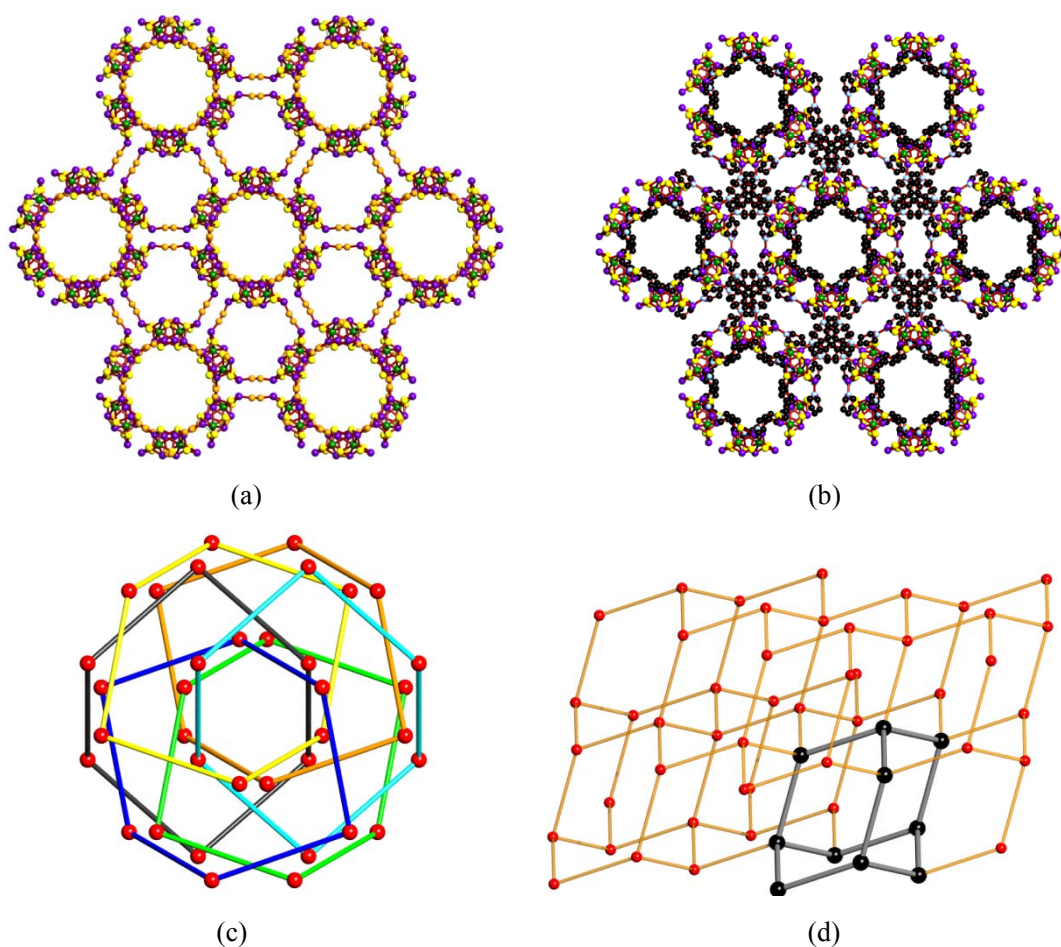
Fig. S2 (a) View of the structure containing $[WS_4Cu_4]^{2+}$ clusters linked by CN^- ions. (b) View of the structure containing $[WS_4Cu_4]^{2+}$ clusters linked by bpea ligands. (c) A schematic representation showing six interpenetrated networks in which $[WS_4Cu_4]^{2+}$ SBUs are linked by the bpea. Each $[WS_4Cu_4]^{2+}$ unit is simplified as a red dot while each bpea linker is simplified as a rod. Each rod color represents one of the six diamond networks. (d) A schematic representation of a single diamond network; an adamantane unit is highlighted. All H atoms are omitted for clarity. Colour code: W green, S yellow, Cu purple, CN light orange, N pale blue, C black.
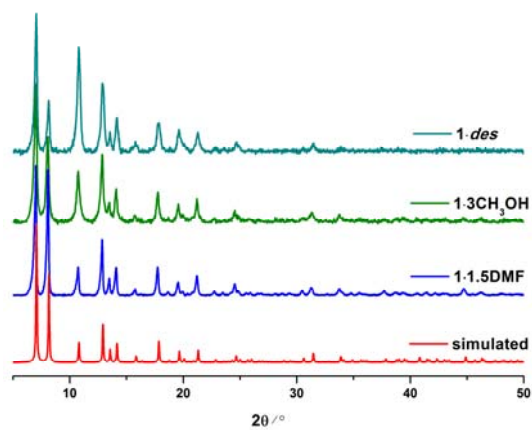
(a)
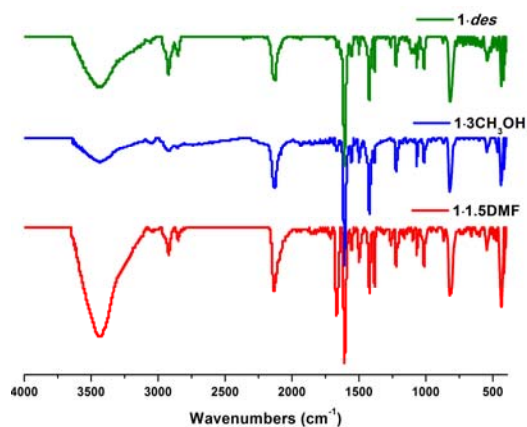
(b)
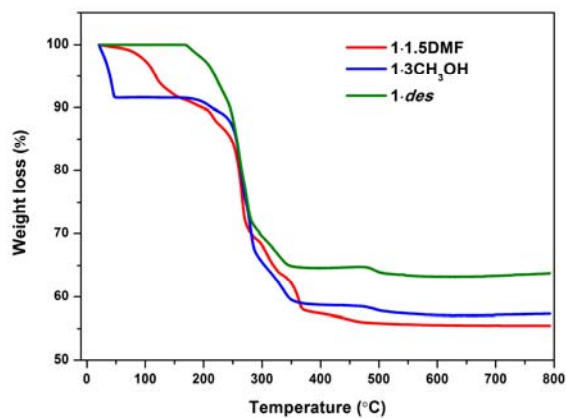
(c)

Fig. S3 (a) PXRD patterns of the simulated (red), as-synthesized **1**·1.5DMF (blue), CH₃OH exchanged **1**·3CH₃OH (green), and the desolvated sample **1**·*des* (atrovirens). (b) IR spectra of as-synthesized **1**·1.5DMF (red), CH₃OH exchanged **1**·3CH₃OH (blue), and the desolvated sample **1**·*des* (green). (c) Thermogravimetric analysis (TGA) curves of as-synthesized **1**·1.5DMF (red), CH₃OH exchanged **1**·3CH₃OH (blue), and the desolvated sample **1**·*des* (green).

Fig. S4 View of a section of one single channel within **1**·1.5DMF. H atoms are omitted for clarity.

Colour code: W green, S yellow, Cu purple, CN light orange, N pale blue, C black.

Fig. S5 Top view of a section of one single channel within **1**·1.5DMF showing the surface of channel of **1**·1.5DMF decorated with phenyl and -CH$_2$- groups. H atoms are omitted for clarity. Colour code: W green, S yellow, Cu purple, CN light orange, N pale blue, C black.
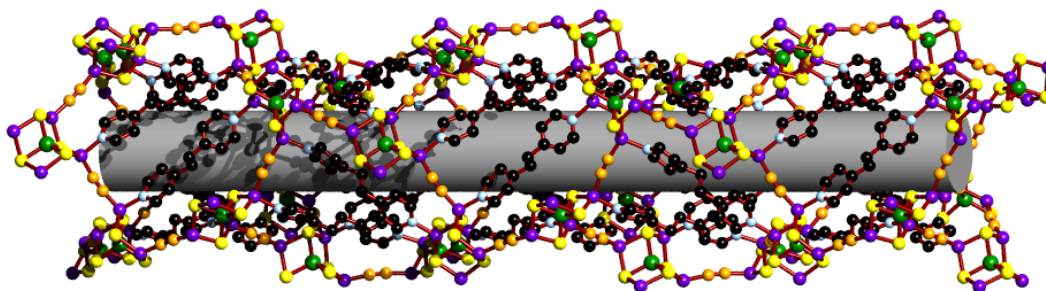

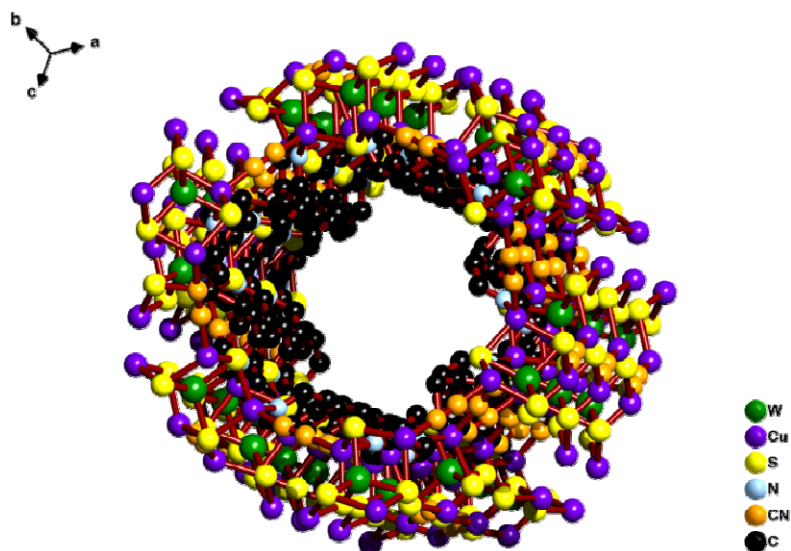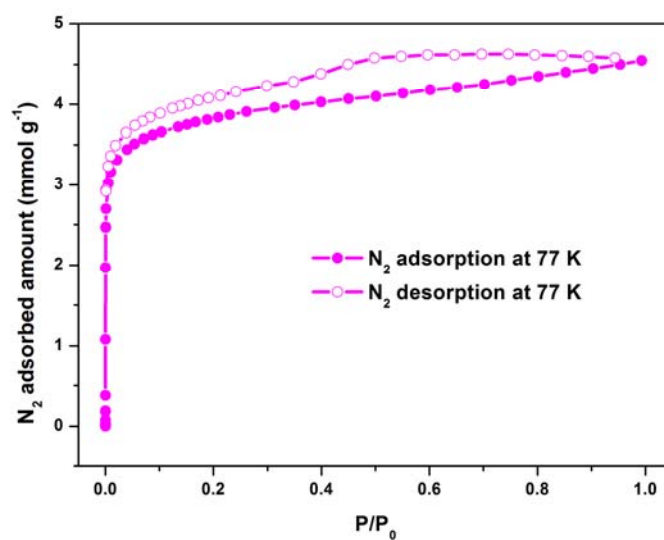**Fig. S6** Nitrogen sorption isotherm of the desolvated sample **1**·*des* at 77 K.

Adsorption experiments.

The removal efficiency was calculated by using the following equation (1):

$$\text{Removal efficiency (\%)} = [(C_i - C_{e\,(t)})/C_i] \times 100 \qquad \textbf{(S1)}$$

The adsorption amount of I_2 was caculated by the following equation (2):

$$Q_{e\,(t)} = V(C_i - C_{e\,(t)})/m \qquad \textbf{(S2)}$$

Where C_i is the initial concentration of I_2 in cyclohexane (mg/L); C_t and C_e are the concentration at time t and at equilibrium (mg/L); Q_t and Q_e are the amount of I_2 adsorbed at time t and equilibrium (mg/g); V is the volume (mL) of the used I_2 solutions; m is the mass of the compound used (g).

Adsorption kinetics models.

The linear form of pseudo-first-order kinetic model is expressed by the following equation (3):

$$\log(Q_e - Q_t) = \log Q_e - (k_1/12.303)t \qquad \textbf{(S3)}$$

The linear form of pseudo-second-order kinetic model is expressed by the following equation (4):

$$t/Q_t = 1/(k_2 Q_e^2) + (1/Q_e)t \qquad \textbf{(S4)}$$

where Q_e (mg/g) and Q_t (mg/g) are the amounts of I_2 adsorbed at equilibrium and at time t (min), respectively; t (min) is adsorption time; k_1 (min^{-1}) and k_2 (g mg^{-1} min^{-1}) is the pseudo-first-order pseudo-second-order adsorption rate constant.

| (a) | (b) |
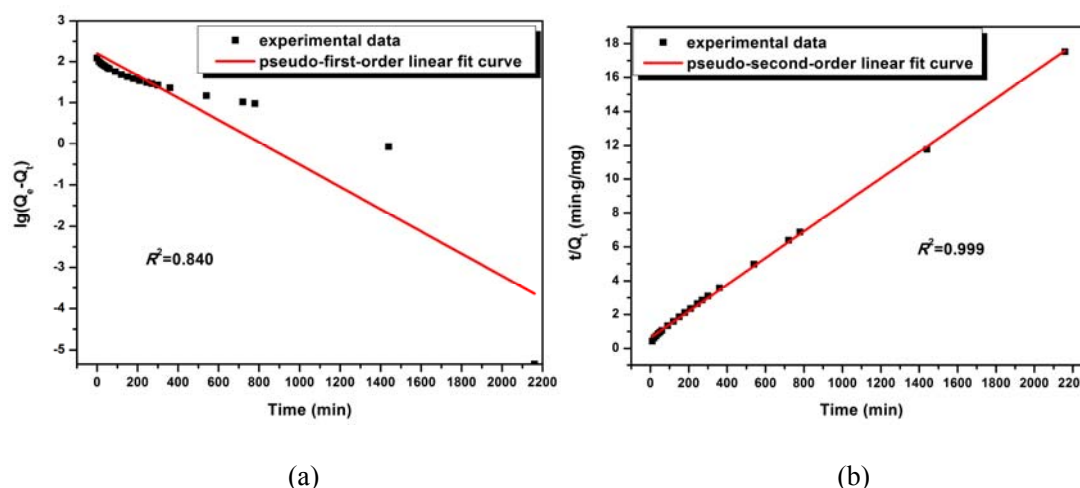
Fig. S7 (a) The pseudo-first-order kinetics and (b) pseudo-second-order kinetics (red) of I_2 removal on **1**·*des* samples (black) (C_i= 2 mM).
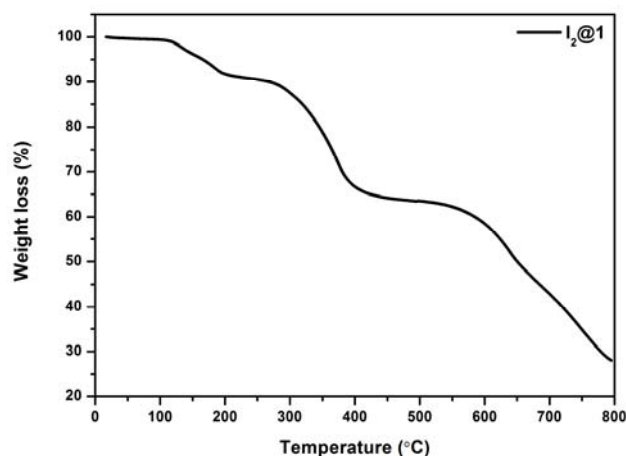
Fig. S8 The TGA curve of $I_2@\mathbf{1}$ sample in cyclohexane solution.

Note: The uptake is 1106 mg iodine per gram of **1**·*des* in cyclohexane to give [WS$_4$Cu$_4$(μ-CN)$_2$(bpea)$_2$]·4.35I$_2$ (**1**·4.35I$_2$, iodine content 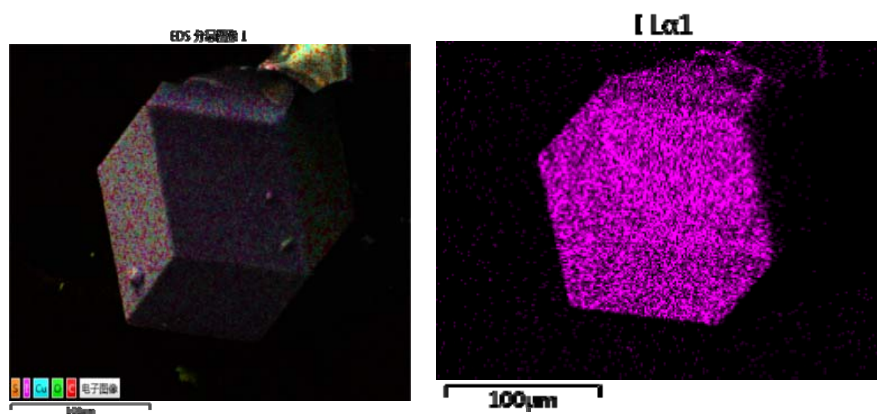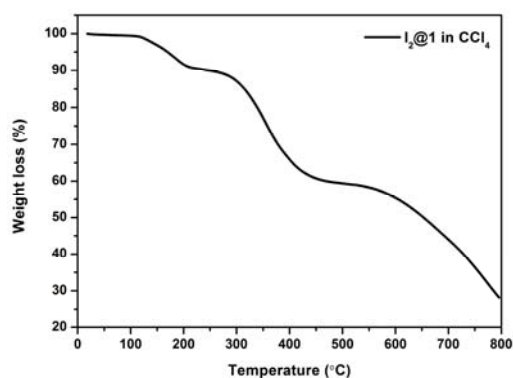of 52.8%, two bpea content of 17.6%, two CN content of 2.49%). Three weight losses are observed from the TGA curve of **1**·4.35I$_2$ (10 °C /min to 800 °C). The first weight loss is due to the leaving of iodine guest molecular with 8.61% up to 207.356 °C and the further weight loss is the decomposition of the compound. The second one is about 26.91% under heating up to 438.94 °C, including 9.31% iodine content. The third one is 36.37% under heating up to 800 °C with 33.88% iodine content. The total weight loss of iodine should be 51.8%, which just slightly less than calculated value of 52.8%. Iodine as an volatile solid, the iodine loaded by the compound 1 seems not easily to remove, which may be due to the strong interaction between iodine and the framework.


Fig. S9 The SEM-mapping images for $I_2@\mathbf{1}$.

**Fig. S10** The TGA curve of I_2@**1** sample in CCl_4 solution.

Note: The uptake is 1.0 g iodine per gram of **1**·*des* in CCl_4 to give $[WS_4Cu_4(\mu\text{-}CN)_2(bpea)_2]\cdot4.08I_2$ (**1**·4.08I_2, iodine content of 51.19%, two bpea content of 18.20%, two CN content of 2.57%). Three weight losses were observed from the TGA curve of **1**·4.08I_2 (10 °C /min to 800 °C). The first weight loss (9.11%) was due to the leaving of iodine guest molecules when it was heated up to 216.53 °C. The second one was ca. 30.89% (including 12.69% iodine content) upon heating up to 471.99 °C. The third one was 31.84% (including 29.27% iodine content) upon heating up to 800 °C. The total weight loss of iodine should be 51.07%, which matched quite well with the calculated value (51.19%).
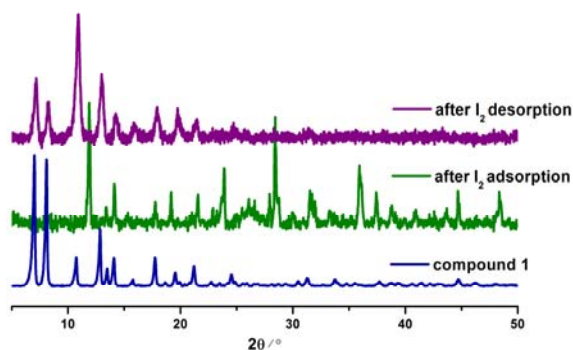
Fig. S11 PXRD patterns of compound **1** (blue), the I_2@**1** sample (green) and the samples after desorption (purple).
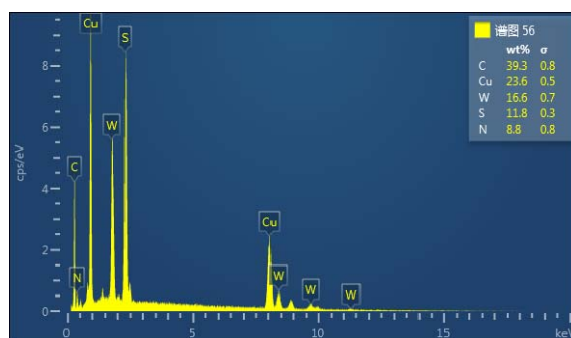
Fig. S12 EDS spectrum of the sample after iodine release.
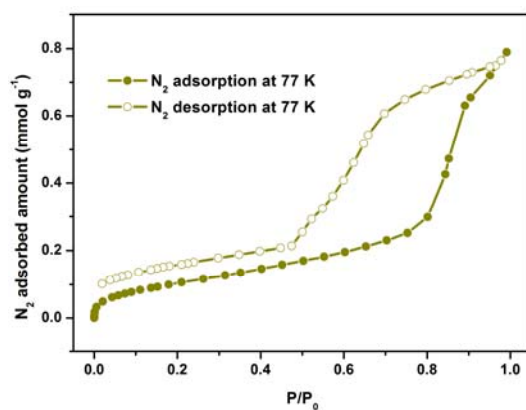
Fig. S13 Nitrogen sorption isotherm of the sample after iodine release at 77 K.

Table S3 Absorption capacities of **1**·*des* and some known materials towards iodine in solution.

Absorbent	Absorption capacity (mg·g^{-1})	Ref.
$Fe_3O_4@PPy$	1627	S6
UiO-66-PYDC[a]	1250	17
$[Cu_4I_3(DABCO)_2]I$[b]	1187	S7
$[WS_4Cu_4(\mu\text{-}CN)_2(bpea)_2]$[c]	1106	This work
$[NH_2(CH_3)_2]\cdot[Zn_4O(BPTC)_2(BDC)_{0.5}]$[d]	1099	S8
$[Zn_3(DLlac)_2(pybz)_2]$[e]	1010	11b
$[CoII_3(lac)_2(pybz)_2]$	900	12c
$[Zn_2(NH_2\text{-}BDC)_2(4\text{-}bpdh)]$[f]	796.6	21
FCMP-600@2[g]	729	S9
$[Cd(ABTC)(H_2O)_2(DMA)]$[h]	680	S10
FCMP-600@1	550	S9
$[(In_3O)_2(Cu_2I_2)_3(ina)_{12}(H_2O)_6](NO_3)_2$[i]	450	S11
$[Zn_9(btc)_4(atz)_{12}]$[j]	395	12a
$MIL\text{-}101\text{-}NH_2$	311	18a

[a] PYDC = pyridine-dicarboxylic acid;

[b] DABCO = *N,N'*-dimethyl-1,4-diazabicyclo[2.2.2]octane;

[c] bpea = 1,2-bis(4-pyridyl)ethane;

[d] H$_3$BPTC = biphenyl-3,4,5-tricarboxylate; H$_2$BDC = terephthalic acid;

[e] DLlac = lactate anion; pybz = 4-pyridylbenzoate;

[f] 4-bpdh = bis(4-pyridyl)-3,4-diaza-2,4-hexadiene;

[g] FCMP = fluorine-enriched conjugated microporous polymers;

[h] H$_4$ABTC = 3,3',5,5'-azobenzenetetracarboxylic acid;

[i] Hina = isonicotinic acid;

[j] btc = 1,3,5-benzenetricarboxylic acid; atz = 5-amino-tetrazole.

References

S1. G. M. Sheldrick, SADABS Empirical Absorption Correction Program; University of Göttingen, Göttingen, Germany.

S2. L. Krause, R. Herbst-Irmer, G. M. Sheldrick and D. Stalke, *J. Appl. Crystallogr.*, 2015, **48**, 3.

S3. R. H. Blessing, *Acta Crystallogr., Sect. A: Found. Crystallogr.*, 1995, **51**, 33.

S4. G. M. Sheldrick, *Acta Crystallogr., Sect. C: Struct. Chem.*, 2015, **71**, 3.

S5. G. R. Fulmer, A. J. M. Miller, N. H. Sherden, H. E. Gottlieb, A. Nudelman, B. M. Stoltz, J. E. Bercaw and K. I. Goldberg, *Organometallics,* 2010, **29**, 2176.

S6. D. K. L. Harijana, V. Chandraa, T. Yoonb and K. S. Kimb, *J. Hazard. Mater.,* 2018, **344**, 576.

S7. B. J. Xin, G. Zeng, L. Gao, Y. Li, S. H. Xing, J. Hua, G. H. Li, Z. Shi and S. H. Feng, *Dalton Trans.,* 2013, **42**, 7562.

S8. W. W. He, S. L. Li, G. S. Yang, Y. Q. Lan, Z. M. Su and Q. Fu, *Chem. Commun.,* 2012, **48**, 10001.

S9. G. Y. Li, C. Yao, J. K. Wang and Y. H. Xu, *Sci. Rep.,* **7**, 13972.

S10. C. Yao, W. Wang, S. R. Zhang, H. Y. Li, Y. H. Xu, Z. M. Su and G. B. Che, *RSC Adv.,* 2018, **8**, 36400.

S11. J. H. Liu, Y. J. Qi, D. Zhao, H. H. Li and S. T. Zheng, *Inorg. Chem.,* 2019, **58**, 516.